

## Supporting Information

### Tuning Humidity Response in 2D MOF Membranes through Nanosheet Geometry

Liangliang Peng<sup>abd</sup>, Zhiqing Lan<sup>b</sup>, Peidong Bao<sup>abd</sup>, Dekai Cai<sup>abd</sup>, Jiangfeng Lu<sup>\*bd</sup> and Gang Xu<sup>bcd</sup>

<sup>a</sup>*College of Chemistry and Materials Science, Fujian Normal University, Fuzhou, Fujian, 350007, P. R. China.*

<sup>b</sup>*State Key Laboratory of Structural Chemistry, and Fujian Provincial Key Laboratory of Materials and Techniques toward Hydrogen Energy, Fujian Institute of Research on the Structure of Matter, Chinese Academy of Sciences, Fuzhou, Fujian 350002, P. R. China.*

<sup>c</sup>*University of Chinese Academy of Science (UCAS), Beijing 100049, P. R. China.*

<sup>d</sup>*Fujian College, University of Chinese Academy of Sciences, Fuzhou, Fujian 350002, P. R. China*

Corresponding author: J Lu (E-mail: [lujiangfeng@fjirsm.ac.cn](mailto:lujiangfeng@fjirsm.ac.cn))

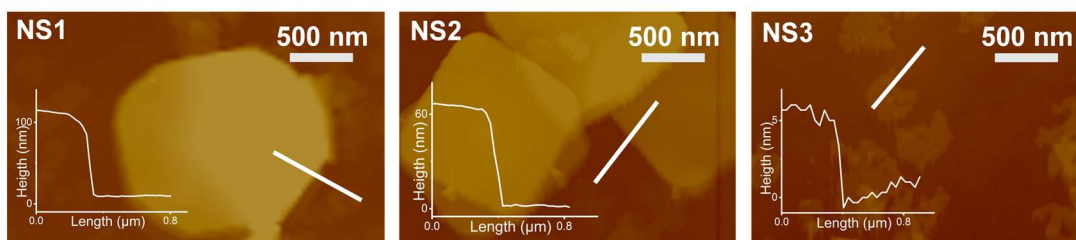


Fig. S1 AFM images of NS1, NS2, and NS3 after ultrasonic treatment.

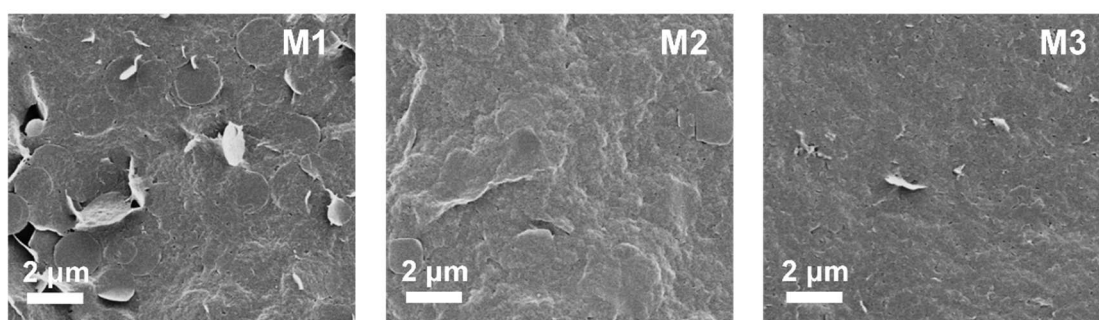


Fig. S2 Top-view SEM images of M1, M2, and M3 membranes.

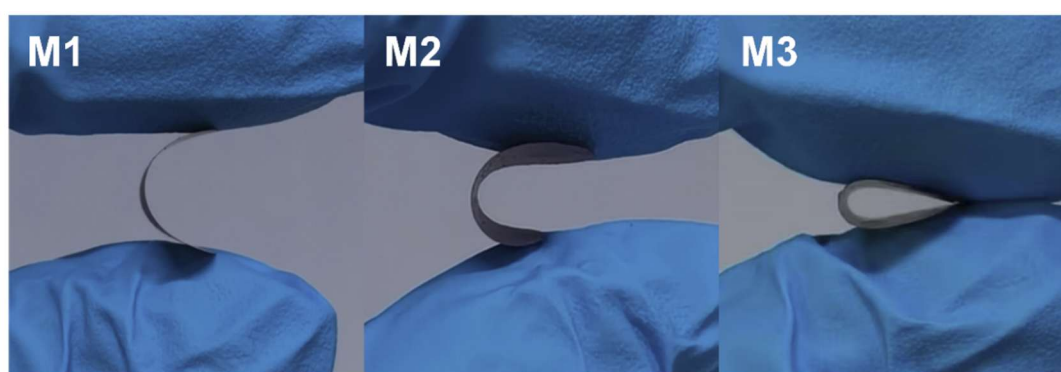


Fig. S3 Side-by-side photographs of free-standing CuTCPP membranes M1-M3 under progressively increased bending deformation, illustrating the different mechanical tolerance limits prior to fracture.

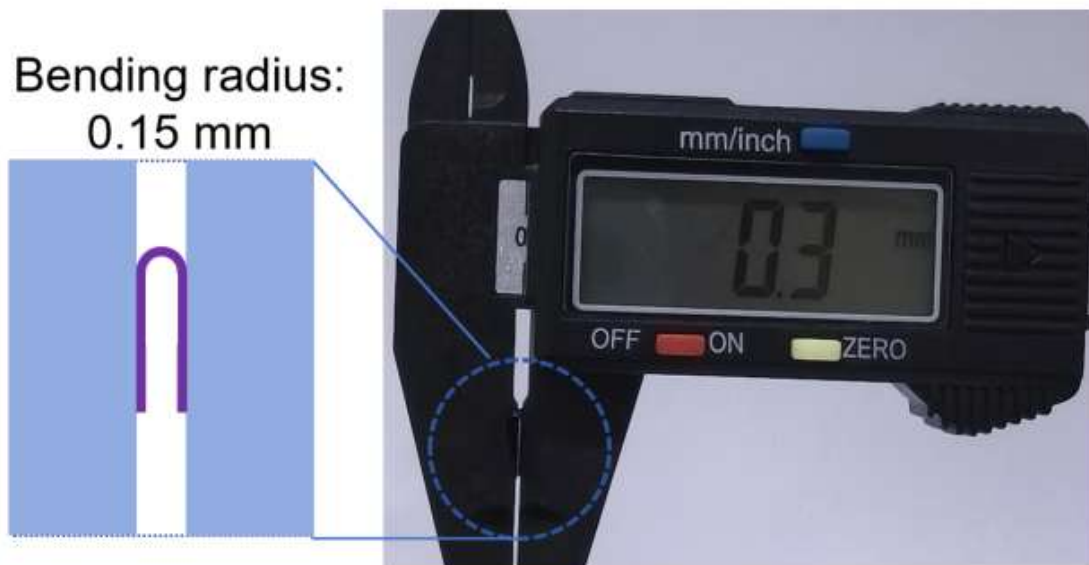


Fig. S4 Optical photograph of the free-standing M3 membrane bent to a curvature radius below 1 mm at a thickness of approximately 11  $\mu\text{m}$ .

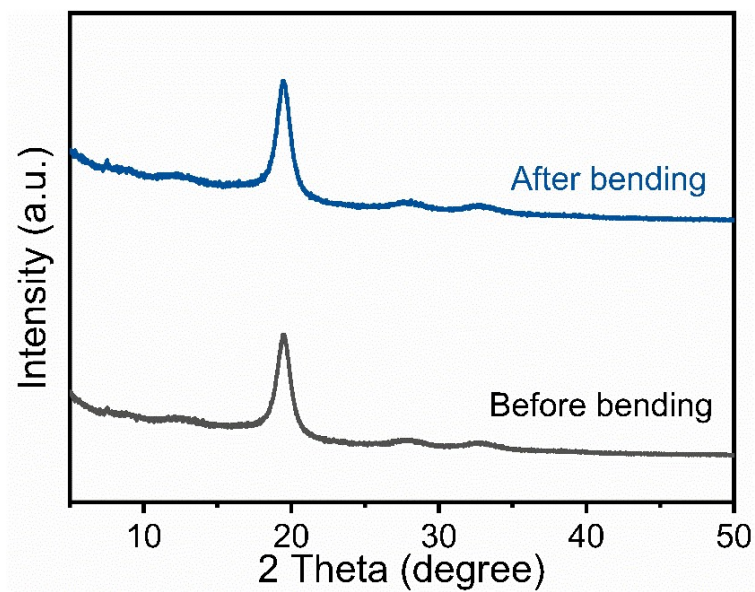


Fig. S5 XRD patterns of the CuTCPP membrane before and after bending.



Fig. S6 Optical image of CuTCPP membrane device.

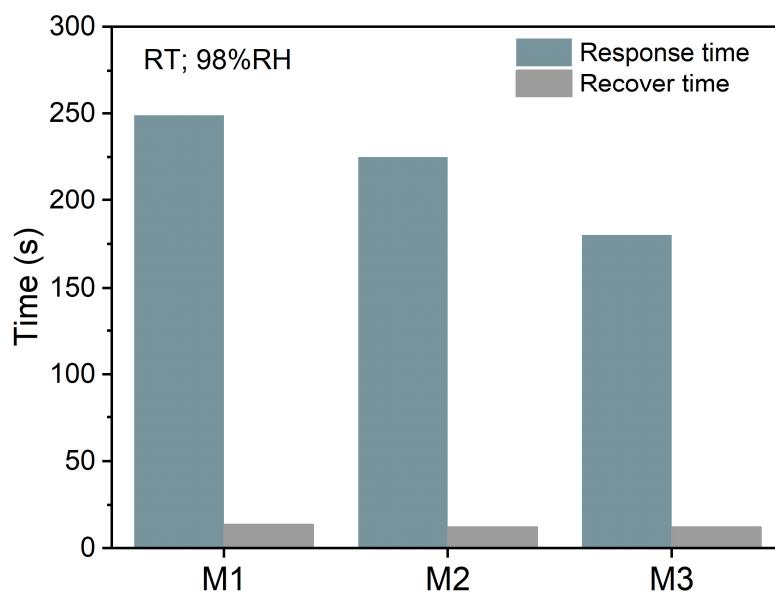


Fig. S7 Response and recovery times of M1, M2, and M3 at 98% RH.

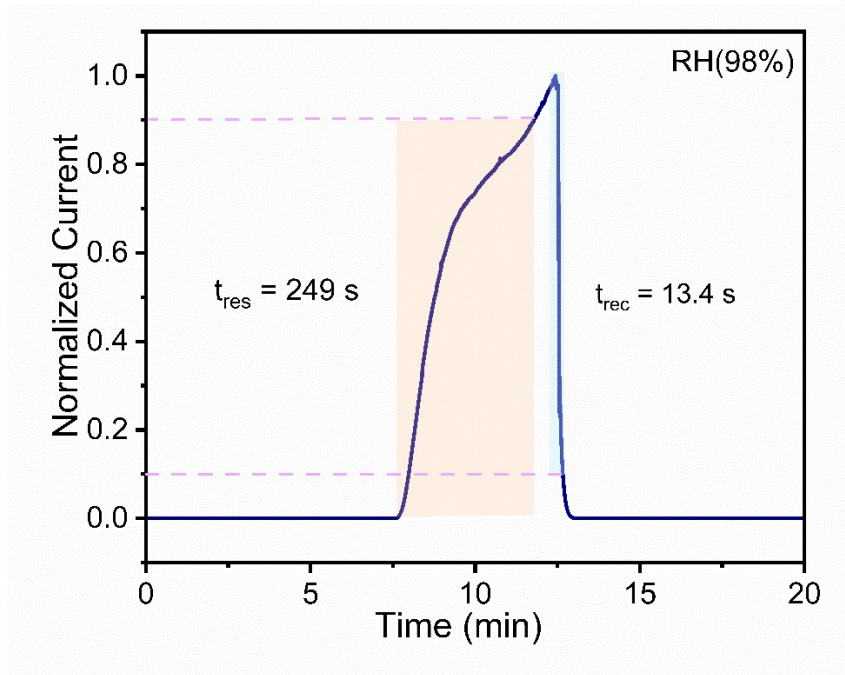


Fig. S8 Response and recovery times of M1 measured at 98% RH.

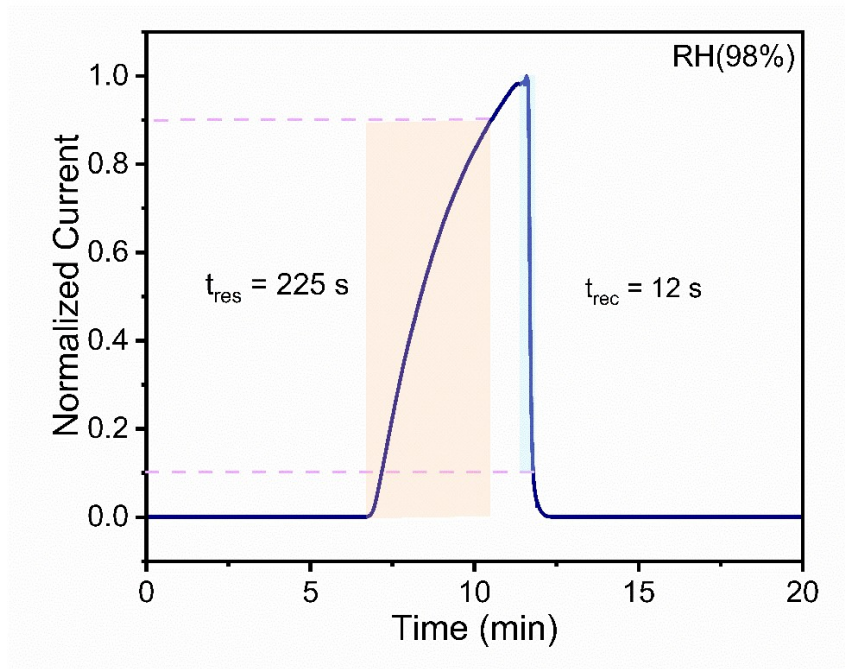


Fig. S9 Response and recovery times of M2 measured at 98% RH.

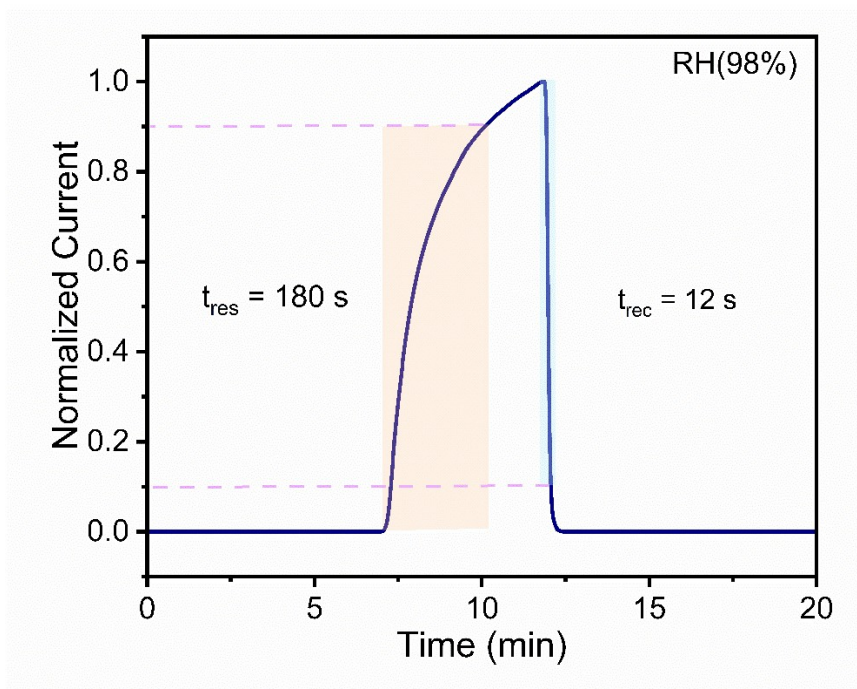


Fig. S10 Response and recovery times of M3 measured at 98% RH.

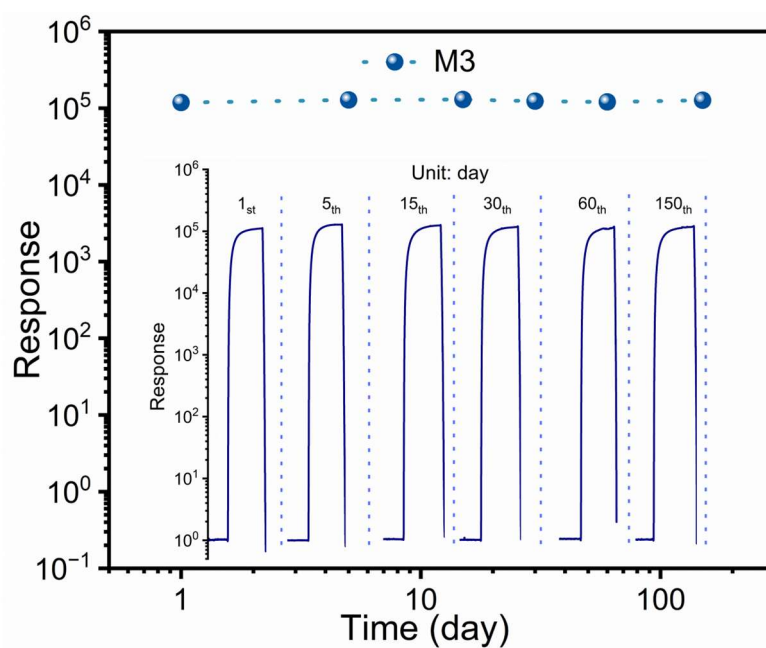


Fig. S11 Long-term stability of M3 membrane under 98% RH.

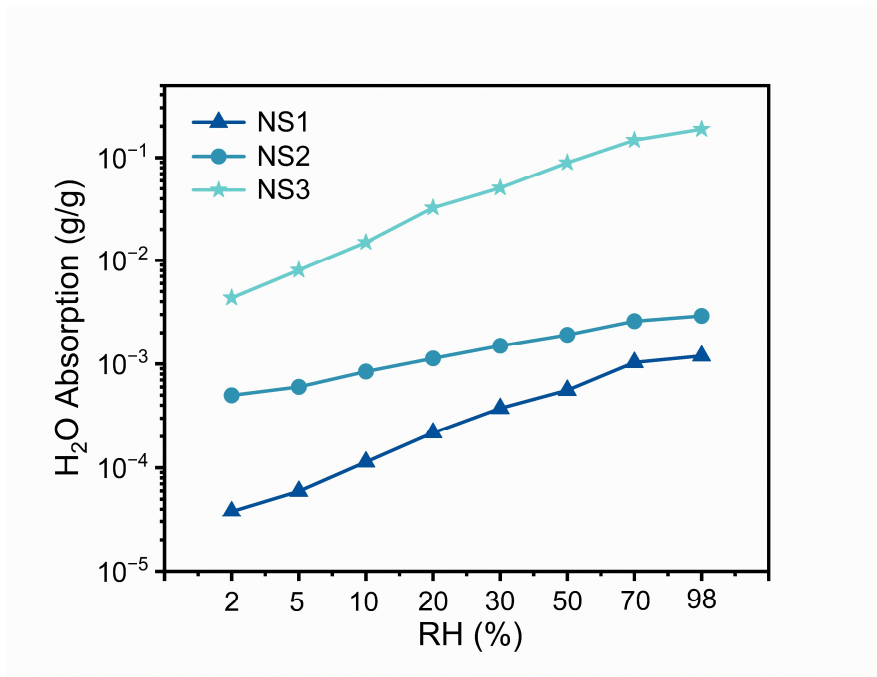


Fig. S12 Dynamic response adsorption curve of CuTCPP nanosheets to water vapor under continuous relative humidity.

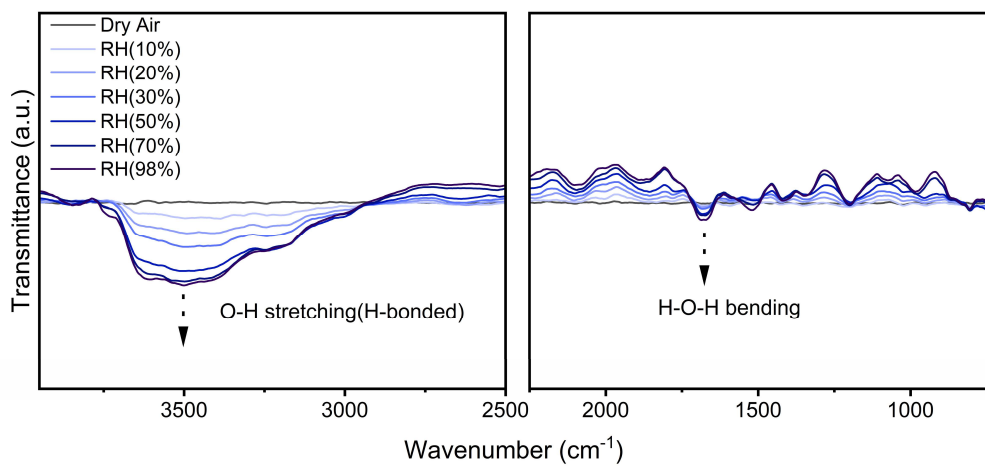


Fig. S13 In situ FTIR spectra of Cu-TCPP M3 membrane under humidity variation.

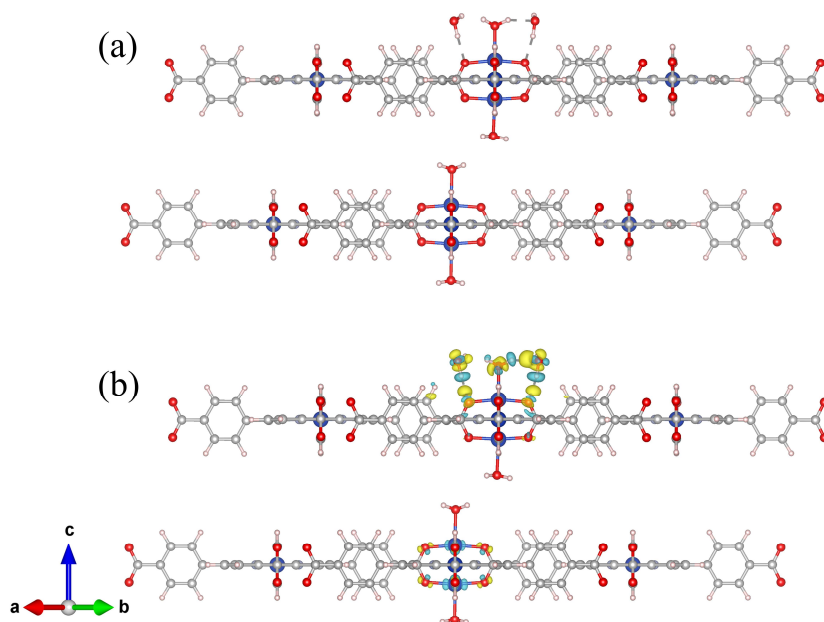


Fig. S14 (a) The model of CuTCPP molecule that absorbs H<sub>2</sub>O molecules; (b) Differential charge density plots of H<sub>2</sub>O molecule adsorbed on CuTCPP. The yellow and green isosurfaces represent electron accumulation and depletion. The isosurface value was set to 0.002e/bohr<sup>3</sup> for H<sub>2</sub>O adsorption.

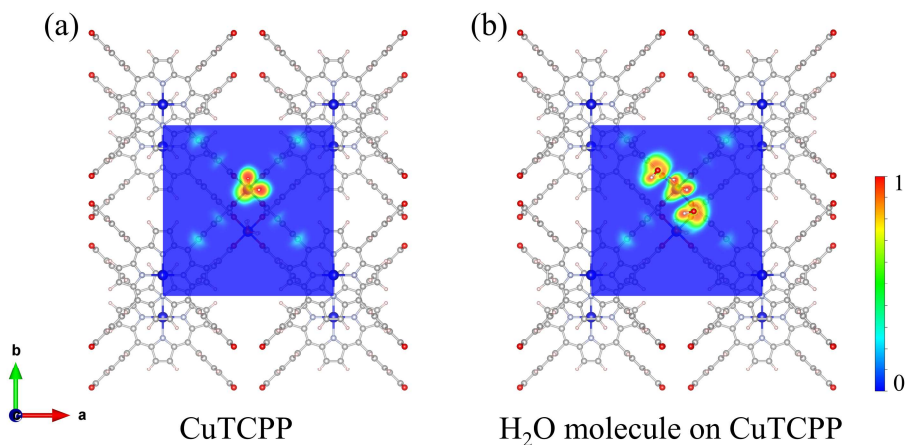


Fig. S15 (a) Slice cutting through O atoms along c-axis of CuTCPP molecule model. (b) Slice cutting through O atoms along c-axis of H<sub>2</sub>O molecule adsorbed on CuTCPP molecule model. Iso-value increases from blue to red, and the maximum electron localization function (ELF) value is scaled to 1.

**Table S1** Thickness, mass, volume, and calculated average density of CuTCPP membranes.

NO.	Thickness	Diameter	Volume	Weight	Density	Average density
M1-1	19.7 $\mu\text{m}$	1.5 cm	$3.48 \times 10^{-3} \text{ cm}^3$	1.8 mg	$0.517 \text{ g}\cdot\text{cm}^{-3}$	0.515 $\text{g}\cdot\text{cm}^{-3}$
M1-2	20.0 $\mu\text{m}$	1.5 cm	$3.54 \times 10^{-3} \text{ cm}^3$	1.9 mg	$0.537 \text{ g}\cdot\text{cm}^{-3}$	
M1-3	20.7 $\mu\text{m}$	1.5 cm	$3.67 \times 10^{-2} \text{ cm}^3$	1.8 mg	$0.492 \text{ g}\cdot\text{cm}^{-3}$	
M2-1	17.7 $\mu\text{m}$	1.5 cm	$3.12 \times 10^{-3} \text{ cm}^3$	2.3 mg	$0.735 \text{ g}\cdot\text{cm}^{-3}$	0.773 $\text{g}\cdot\text{cm}^{-3}$
M2-2	18.7 $\mu\text{m}$	1.5 cm	$3.30 \times 10^{-3} \text{ cm}^3$	2.2 mg	$0.666 \text{ g}\cdot\text{cm}^{-3}$	
M2-3	16.3 $\mu\text{m}$	1.5 cm	$2.90 \times 10^{-3} \text{ cm}^3$	2.3 mg	$0.795 \text{ g}\cdot\text{cm}^{-3}$	
M3-1	10.7 $\mu\text{m}$	1.5 cm	$1.89 \times 10^{-3} \text{ cm}^3$	2.0 mg	$1.059 \text{ g}\cdot\text{cm}^{-3}$	1.029 $\text{g}\cdot\text{cm}^{-3}$
M3-2	11.7 $\mu\text{m}$	1.5 cm	$2.06 \times 10^{-3} \text{ cm}^3$	2.0 mg	$0.968 \text{ g}\cdot\text{cm}^{-3}$	
M3-3	10.7 $\mu\text{m}$	1.5 cm	$1.89 \times 10^{-3} \text{ cm}^3$	2.0 mg	$1.059 \text{ g}\cdot\text{cm}^{-3}$	

**Table S2** State-of-the-art 2D sensing materials for chemiresistive humidity sensor at RT.

Sensing materials	Response range (RH)	Response%/RH%	Ref.
Cu-TCPP	2-98	$1.3 \times 10^7/98$	This work
Graphene	8-95	110/88	1
GNCP	10-97	$2.0 \times 10^6/97$	2
GQD	8-97	$1.4 \times 10^5/97$	3
Defect graphene	3-30	330/30	4
Borophene–Graphene	11-85	$4.2 \times 10^3/85$	5
$\alpha'$ -4H borophene	67-85	$1.5 \times 10^4/85$	5
Graphene/Ag	12-97	35/97	6
Borophene–MoS <sub>2</sub>	11-97	$1.6 \times 10^4/97$	7
GO	10-80	$1 \times 10^3/80$	8
RGO	4.3-75.7	6/75.7	9
rGO/MoS <sub>2</sub>	5-85	$2.5 \times 10^3/85$	10
g-C <sub>3</sub> N <sub>4</sub>	11-97	$3.5 \times 10^5/97$	11
CuCl <sub>2</sub> -MOF-303	33-95	$5.6 \times 10^4/95$	12
CMC-Na/MOF-801/PPY	7-85	$1.24 \times 10^5/85$	13
CoTCPP@PA	23-95	$2 \times 10^5/95$	14
HTT–Pb	5-100	$6 \times 10^6/90$	15
MoS <sub>2</sub>	5-35	$6 \times 10^6/35$	16
Ti <sub>3</sub> C <sub>2</sub> Tx	11-98	$6.0 \times 10^3/95$	17
BP	10-85	$1.0 \times 10^6/85$	18

## References

- 1 S. Andrić, T. Tomašević-Ilić, M. V. Bošković, M. Sarajlić, D. Vasiljević-Radović, M. M. Smiljanić and M. Spasenović, *Nanotechnology*, 2021, **32**, 025505.
- 2 J. He, P. Xiao, J. Shi, Y. Liang, W. Lu, Y. Chen, W. Wang, P. Théato, S.-W. Kuo and T. Chen, *Chem. Mater.*, 2018, **30**, 4343–4354.
- 3 T. Alizadeh and M. Shokri, *Sens. Actuators B Chem.*, 2016, **222**, 728–734.
- 4 Q. Huang, D. Zeng, S. Tian and C. Xie, *Mater. Lett.*, 2012, **83**, 76–79.
- 5 C. Hou, G. Tai, B. Liu, Z. Wu and Y. Yin, *Nano Res.*, 2021, **14**, 2337–2344.
- 6 Y. Pang, J. Jian, T. Tu, Z. Yang, J. Ling, Y. Li, X. Wang, Y. Qiao, H. Tian, Y. Yang and T.-L. Ren, *Biosens. Bioelectron.*, 2018, **116**, 123–129.
- 7 C. Hou, G. Tai, Y. Liu, Z. Wu, Z. Wu and X. Liang, *J. Mater. Chem. A*, 2021, **9**, 13100–13108.
- 8 A. De Luca, S. Santra, R. Ghosh, S. Z. Ali, J. W. Gardner, P. K. Guha and F. Udrea, *Nanoscale*, 2016, **8**, 4565–4572.
- 9 X. Wang, Z. Xiong, Z. Liu and T. Zhang, *Adv. Mater.*, 2015, **27**, 1370.
- 10 S. Y. Park, Y. H. Kim, S. Y. Lee, W. Sohn, J. E. Lee, D. H. Kim, Y.-S. Shim, K. C. Kwon, K. S. Choi, H. J. Yoo, J. M. Suh, M. Ko, J.-H. Lee, M. J. Lee, S. Y. Kim, M. H. Lee and H. W. Jang, *J. Mater. Chem. A*, 2018, **6**, 5016–5024.
- 11 W. Meng, S. Wu, X. Wang and D. Zhang, *Sens. Actuators B Chem.*, 2020, **315**, 128058.
- 12 K. Wu, L. Guo, W. Wang, Z. Yang and H. Liu, *Sens. Actuators B Chem.*, 2024, **417**, 136174.
- 13 Wu K., He Q. and Liu H., *Acta Phys. Sin.*, 2026, **75**, 040803.
- 14 Y. Huo, M. Bu, Z. Ma, J. Sun, Y. Yan, K. Xiu, Z. Wang, N. Hu and Y.-F. Li, *J. Colloid Interface Sci.*, 2022, **607**, 2010–2018.
- 15 J. Huang, Y. He, M.-S. Yao, J. He, G. Xu, M. Zeller and Z. Xu, *J. Mater. Chem. A*, 2017, **5**, 16139-16143.
- 16 J. Zhao, N. Li, H. Yu, Z. Wei, M. Liao, P. Chen, S. Wang, D. Shi, Q. Sun and G. Zhang, *Adv. Mater.*, 2017, **29**, 1702076.
- 17 Z. Yang, A. Liu, C. Wang, F. Liu, J. He, S. Li, J. Wang, R. You, X. Yan, P. Sun, Y. Duan and G. Lu, *ACS Sens.*, 2019, **4**, 1261-1269.
- 18 P. Yasaei, A. Behranginia, T. Foroozan, M. Asadi, K. Kim, F. Khalili-Araghi and A. Salehi-Khojin, *ACS Nano*, 2015, **9**, 9898–9905.